

## RESEARCH ARTICLE

# Discordant Alzheimer's neurodegenerative biomarkers and their clinical outcomes

Yu Guo<sup>1</sup>, Hong-Qi Li<sup>2</sup>, Lin Tan<sup>1</sup>, Shi-Dong Chen<sup>2</sup>, Yu-Xiang Yang<sup>2</sup>, Ya-Hui Ma<sup>1</sup>, Chuan-Tao Zuo<sup>3</sup>, Qiang Dong<sup>2</sup>, Lan Tan<sup>1</sup>, Jin-Tai Yu<sup>2</sup>  & Alzheimer's Disease Neuroimaging Initiative<sup>a</sup>

<sup>1</sup>Department of Neurology, Qingdao Municipal Hospital Affiliated to Qingdao University, Qingdao, China

<sup>2</sup>Department of Neurology and Institute of Neurology, Huashan Hospital, Shanghai Medical College, Fudan University, Shanghai, China

<sup>3</sup>PET Center, Huashan Hospital, Fudan University, Shanghai, China

## Correspondence

Jin-Tai Yu, Department of Neurology and Institute of Neurology, Huashan Hospital, Shanghai Medical College, Fudan University, 12th Wulumuqi Zhong Road, Shanghai 200040, China. Tel: +86 21 52888160; Fax: +86 21 62483421; E-mail: jintai\_yu@fudan.edu.cn

## Funding Information

This study was supported by grants from the National Key R&D Program of China (2018YFC1314700), the National Natural Science Foundation of China (91849126), Shanghai Municipal Science and Technology Major Project (No.2018SHZDZX03) and ZJlab, Tianqiao and Chrissy Chen Institute, and the State Key Laboratory of Neurobiology and Frontiers Center for Brain Science of Ministry of Education, Fudan University. Data collection and sharing for this project were funded by the Alzheimer's Disease Neuroimaging Initiative (ADNI) (National Institutes of Health Grant U01 AG024904) and DOD ADNI (Department of Defense award number W81XWH-12-2-0012). ADNI is funded by the National Institute on Aging, the National Institute of Biomedical Imaging and Bioengineering, and through generous contributions from the following: AbbVie, Alzheimer's Association; Alzheimer's Drug Discovery Foundation; Araclon Biotech; BioClinica, Inc.; Biogen; Bristol-Myers Squibb Company; CereSpir, Inc.; Cogstate; Eisai Inc.; Elan Pharmaceuticals, Inc.; Eli Lilly and Company; EuroImmun; F. Hoffmann-La Roche Ltd and its affiliated company Genentech, Inc.; Fujirebio; GE Healthcare; IXICO Ltd.; Janssen Alzheimer Immunotherapy Research & Development, LLC.; Johnson & Johnson Pharmaceutical Research & Development LLC.; Lumosity; Lundbeck; Merck & Co., Inc.; Meso Scale

## Abstract

**Objective:** In the 2018 ATN framework, Alzheimer's neurodegenerative biomarkers comprised cerebrospinal fluid (CSF) total tau, <sup>18</sup>F-fluorodeoxyglucose-positron emission tomography, and brain atrophy. We aimed to assess the clinical outcomes of having discordant Alzheimer's neurodegenerative biomarkers. **Methods:** A total of 721 non-demented individuals from the Alzheimer's Disease Neuroimaging Initiative database were included and then further categorized into concordant-negative, discordant, and concordant-positive groups. Demographic distributions of the groups were compared. Longitudinal changes in clinical outcomes and risk of conversion were assessed using linear mixed-effects models and multivariate Cox proportional hazard models, respectively. **Results:** Discordant group was intermediate to concordant-negative and concordant-positive groups in terms of *APOE*  $\epsilon$ 4 positivity, CSF amyloid-beta, and phosphorylated tau. Compared with concordant-negative group, discordant group deteriorated faster in cognitive scores (Mini-Mental State Examination, the Clinical Dementia Rating-Sum of Boxes, and the Functional Activities Questionnaire) and demonstrated greater rates of atrophy in brain structures (hippocampus, entorhinal cortex, and whole brain), and concordant-positive group performed worse over time than discordant group. Moreover, the risk of cognitive decline increased from concordant-negative to discordant to concordant-positive. The results from longitudinal analyses were validated in A+T+, cognitively normal, and mild cognitive impairment individuals, and were also validated by applying different cutoffs and neurodegenerative biomarkers. **Interpretation:** Discordant neurodegenerative status denotes a stage of cognitive function which is intermediate between concordant-negative and concordant-positive. Identification of discordant cases would provide insights into intervention and new therapy approaches, particularly in A+T+ individuals. Moreover, this work may be a complement to the ATN scheme.

Diagnostics, LLC.; NeuroRx Research; Neurotrack Technologies; Novartis Pharmaceuticals Corporation; Pfizer Inc.; Piramal Imaging; Servier; Takeda Pharmaceutical Company; and Transition Therapeutics. The Canadian Institutes of Health Research is providing funds to support ADNI clinical sites in Canada. Private sector contributions are facilitated by the Foundation for the National Institutes of Health ([www.fnih.org](http://www.fnih.org)). The grantee organization is the Northern California Institute for Research and Education, and the study is coordinated by the Alzheimer's Therapeutic Research Institute at the University of Southern California. ADNI data are disseminated by the Laboratory for Neuro Imaging at the University of Southern California.

Received: 15 May 2020; Revised: 8 August 2020; Accepted: 25 August 2020

***Annals of Clinical and Translational Neurology* 2020; 7(10): 1996–2009**

doi: 10.1002/acn3.51196

<sup>a</sup>Data used in preparation of this article were obtained from the Alzheimer's Disease Neuroimaging Initiative (ADNI) database ([adni.loni.usc.edu](http://adni.loni.usc.edu)). As such, the investigators within the ADNI contributed to the design and implementation of ADNI and/or provided data but did not participate in analysis or writing of this report. A complete listing of ADNI investigators can be found at: [http://adni.loni.usc.edu/wp-content/uploads/how\\_to\\_apply/ADNI\\_Acknowledgement\\_List.pdf](http://adni.loni.usc.edu/wp-content/uploads/how_to_apply/ADNI_Acknowledgement_List.pdf).

## Introduction

In 2018, the National Institute on Aging-Alzheimer's Association (NIA-AA) created a research framework to biologically define Alzheimer's disease (AD) by “ATN” biomarkers (amyloid-beta ( $A\beta$ ) deposition [“A”], pathologic tau [“T”], and neurodegeneration [“N”]), and treated cognitive impairment as a symptom/sign of the disease.<sup>1</sup> In this system, “N” biomarkers are indicators of neurodegeneration or neuronal injury based on elevated cerebrospinal fluid (CSF) total tau (t-tau), hypometabolism on <sup>18</sup>F-fluorodeoxyglucose-positron emission tomography (FDG-PET), or brain atrophy on magnetic resonance image (MRI).<sup>1</sup>

Neurodegeneration, especially synapse loss, is the aspect of AD neuropathological changes that is most closely

related to symptoms.<sup>2</sup> The “N” biomarker panel provides vital pathological staging information<sup>1</sup> and exploring these biomarkers in actual research is necessary. Although the three “N” biomarkers can be used interchangeably, it is worth noting that heterogeneity exists among them.<sup>3–5</sup> CSF t-tau probably shows the intensity of neuronal damage at a specific time point<sup>3,6–8</sup>; brain atrophy on MRI reveals cumulative loss and shrinkage of the neuropil<sup>9–11</sup>; and FDG-PET may reflect atrophy of the neuropil and impaired function of neurons. All these differences among “N” biomarkers likely lead to discordance.<sup>5,12–15</sup> Discordant biomarkers potentially have significant implications for neurobiological mechanisms of biomarker discrepancies and AD neuropathogenesis.<sup>16</sup> Biomarker discordance has been examined between CSF  $A\beta$  and  $A\beta$  PET,<sup>16,17</sup> as well as between CSF phosphorylated tau (p-tau) and tau

PET.<sup>18</sup> Prior studies mainly focused on the associations of neurodegenerative biomarkers or only a single biomarker rather than investigations into the combination of multiple neurodegenerative markers utilizing various modalities.<sup>18–22</sup> However, whether and how “N” biomarker discordance affects clinical outcomes are currently understudied. Herein, we conducted the first longitudinal study to compare the discordant group with concordant-negative and concordant-positive groups in terms of baseline demographic distributions and longitudinal clinical outcomes.

## Methods

### Alzheimer’s Disease Neuroimaging Initiative (ADNI) study design

Data used in the preparation of this article were obtained from the ADNI database (<http://adni.loni.usc.edu>).<sup>23,24</sup> The ADNI was launched in 2003 as a public–private partnership with the primary goal of testing the effectiveness of integrating neuroimaging, clinical, biological, and neuropsychological markers in measuring the progression of mild cognitive impairment (MCI) and early AD. All ADNI participants have been recruited from more than 50 sites across the United States and Canada.

### Participants

Subjects from the ADNI prospective clinical cohort were included in this article if they received baseline and follow-up clinical, neuropsychological, and CSF assessments as well as MRI and FDG-PET examinations. ADNI participants were followed longitudinally, with visits every 3 months for the first year, followed by half-year visits. At each follow-up visit, any change to a participant’s clinical diagnosis or biomarker data was recorded in the ADNI database. To avoid the impact of AD on results, we included only non-demented subjects diagnosed as cognitively normal (CN) controls and MCI patients. For detailed diagnostic criteria, see [www.adni-info.org](http://www.adni-info.org).

### CSF measurements

CSF samples were collected and shipped on dry ice to the ADNI Biomarker core laboratory at the University of Pennsylvania Medical Center. Aliquots (0.5 mL) were prepared from these samples and stored in barcode-labeled polypropylene vials at  $-80^{\circ}\text{C}$ . The CSF proteins, including CSF A $\beta$ 42, p-tau, and t-tau, were measured using the multiplex xMAP Luminex platform (Luminex Corp, Austin, TX) with the INNOCIA AlzBio3 kit (Innogenetics).<sup>25</sup>

## Neuroimaging and cognition

Structural MRI brain scans were acquired by Siemens Trio 3.0 T or Vision 1.5 T scanners. Automated volume measures were obtained with FreeSurfer (<http://surfer.nmr.mgh.harvard.edu/fswiki>). Our study used averaged volume measurements for hippocampus, entorhinal cortex, and whole brain. The estimated total intracranial volume (eTIV) was applied to adjust the hippocampal volume (HPV) with the following equation: adjusted hippocampal volume (aHPV) = Raw HPV - b (eTIV - Mean eTIV), where b indicated the regression coefficient when HPV was regressed against eTIV.<sup>26</sup> And we applied the calculated aHPV as a marker of neurodegeneration.

FDG-PET data were derived from UC Berkeley and Lawrence Berkeley National Laboratory. A detailed description of FDG-PET image acquisition and processing can be found at <http://adni.loni.usc.edu/data-samples/pet/>. Mean FDG uptake was averaged over five predefined regions of interest (metaROIs) that are sensitive to AD-related changes in metabolism, including right and left angular gyri, right and left inferior temporal regions, and bilateral posterior cingulate. PET images were spatially normalized in Statistical Parametric Mapping (SPM) to the MNI PET template. We extracted the mean counts from the five metaROIs for each subject’s FDG scans at each time point, computing the intensity values with SPM subroutines. Finally, the intensity of each metaROI mean was normalized via dividing it by pons/vermis reference region mean.

Cognition assessments were completed by Mini-Mental State Examination (MMSE), Clinical Dementia Rating Scale-Sum of Boxes (CDRSB), and Functional Activities Questionnaire (FAQ) scores.

### Grouping of subjects

Group classifications were determined by normal (–) and abnormal (+) biomarker results at baseline. Based on the cutoff thresholds of biomarkers reported in previous articles, the cutoff concentrations of CSF A $\beta$ 42 and p-tau were 192 pg/mL and 23 pg/mL, respectively.<sup>27</sup> A+T+ subjects were those who had CSF A $\beta$ 42 levels  $\leq 192$  pg/mL and p-tau levels  $\geq 23$  pg/mL. CSF t-tau-positive (N+) referred to the levels  $\geq 93$  pg/mL.<sup>27</sup> The aHPV-positive (N+) was defined as the cutoff point  $\leq 6723$  mm<sup>3</sup>.<sup>26</sup> According to the standard uptake value ratio (SUVr), we defined FDG-PET-positive (N+) and negative (N–) subjects based on a cutoff point of 1.21.<sup>27</sup>

In this article, we performed sensitivity analyses using different cutoffs. Firstly, we excluded a total of 341 borderline values within  $\pm 5\%$  of the above cutoff value (Appendix S1), to avoid drawing conclusions based on

**Table 1.** Baseline demographic characteristics.

Characteristics	CSF/PET group			CSF/MRI group			PET/MRI group		
	CSF-/PET-	Discordant	CSF+/PET+	CSF-/MRI-	Discordant	CSF+/MRI+	PET-/MRI-	Discordant	PET+/MRI+
N (%)	394 (54.6)	238 (33.0)	89 (12.3)	387 (53.7)	247 (34.3)	87 (12.1)	392 (54.4)	223 (30.9)	106 (14.7)
Baseline C-IMCI (%)	187 (47.5) / 207 (52.5)	77 (32.4) / 161 (67.6)	15 (16.9) / 74 (83.1)	199 (51.4) / 188 (48.6)	68 (27.5) / 179 (72.5)	12 (13.8) / 75 (86.2)	200 (51.0) / 192 (49.0)	67 (30.0) / 156 (70.0)	12 (11.3) / 94 (88.7)
Age (years)	71.31 (6.54)	74.03 (6.64)	73.80 (7.15)	70.79 (6.32)	73.89 (6.87)	76.30 (6.04)	70.81 (6.48)	74.24 (6.68)	75.19 (6.26)
Female (%)	189 (48.0)	106 (44.5)	40 (44.9)	180 (46.5)	110 (44.5)	45 (51.7)	203 (51.8)	86 (38.6)	46 (43.4)
Years of education	16.41 (2.60)	15.95 (2.70)	16.24 (2.88)	16.41 (2.51)	16.00 (2.87)	16.14 (2.78)	16.27 (2.58)	16.34 (2.67)	15.90 (3.02)
APOE ε4 positive (%)	115 (29.2)	116 (48.7)	63 (70.8)	120 (31.0)	115 (46.6)	59 (67.8)	132 (33.7)	93 (41.7)	69 (65.1)
MMSE	28.71 (1.36)	28.13 (1.73)	27.36 (1.90)	28.78 (1.31)	28.07 (1.73)	27.26 (1.88)	28.73 (1.38)	28.24 (1.64)	27.21 (1.86)
CDRSB	0.63 (0.76)	1.12 (1.05)	1.55 (1.08)	0.62 (0.77)	1.11 (1.02)	1.60 (1.07)	0.59 (0.74)	1.11 (1.02)	1.63 (1.06)
FAQ	1.07 (2.42)	2.49 (3.97)	3.94 (3.87)	0.99 (2.37)	2.60 (3.82)	3.85 (4.23)	0.82 (2.03)	2.71 (3.91)	4.10 (4.32)
aHPV (mm <sup>3</sup> )	7500.63 (921.10)	6839.52 (1041.09)	6541.08 (960.61)	7766.55 (639.69)	6680.60 (987.30)	5855.68 (599.13)	7781.43 (649.76)	6717.42 (879.79)	5819.82 (713.19)
Entorhinal volume (mm <sup>3</sup> )	3827.71 (620.04)	3585.14 (734.22)	3376.54 (656.79)	3917.81 (562.59)	3521.44 (714.07)	3151.51 (652.21)	3911.49 (584.37)	3562.40 (643.56)	3124.30 (725.46)
Whole brain volume (mm <sup>3</sup> )	1064460.52 (100370.91)	1037127.34 (108952.95)	1026394.86 (94248.31)	1070554.08 (99378.09)	1035742.30 (104031.28)	1005309.84 (98989.66)	1067953.92 (100157.81)	1039788.25 (98088.90)	1010176.21 (113359.18)
FDG-PET	1.34 (0.09)	1.22 (0.13)	1.12 (0.07)	1.31 (0.12)	1.25 (0.13)	1.20 (0.13)	1.35 (0.09)	1.23 (0.12)	1.11 (0.07)
CSF Aβ42 (pg/mL)	201.85 (48.10)	165.69 (51.21)	141.74 (37.08)	202.97 (47.95)	164.22 (49.19)	143.27 (42.20)	196.77 (50.60)	175.56 (51.55)	144.26 (41.16)
CSF p-tau (pg/mL)	29.61 (14.75)	41.85 (22.89)	58.92 (23.11)	28.97 (14.45)	45.19 (25.63)	51.63 (16.79)	34.74 (20.14)	37.63 (22.37)	45.83 (21.05)
CSF t-tau (pg/mL)	56.21 (17.76)	94.17 (47.92)	144.48 (43.32)	55.09 (17.81)	94.95 (45.21)	145.37 (45.97)	69.52 (37.62)	85.42 (46.28)	104.88 (56.06)

Continuous variables were presented as means (standard deviations (SDs)), and categorical variables were presented as numbers (percentages). Discordant group in the CSF/PET, CSF/MRI, and PET/MRI represent combined group of CSF-/PET+ and CSF+/PET-, combined group of CSF-/MRI- and CSF+/MRI+, and combined group of PET-/MRI- and PET+/MRI+, respectively. Abbreviations: aHPV, adjusted hippocampal volume; Aβ, amyloid beta; CDRSB, Clinical Dementia Rating Scale-Sum of Boxes; CN, cognitively normal; CSF, cerebrospinal fluid; FAQ, Functional Activities Questionnaire; FDG, <sup>18</sup>F-fluorodeoxyglucose; MCI, mild cognitive impairment; MMSE, Mini-Mental State Examination; MRI, Magnetic Resonance Imaging; PET, positron emission tomography; p-tau, phosphorylated tau; t-tau, total tau.

borderline cases that easily could be misclassified due to variable measurements. The cut-offs used in the article were thus: CSF t-tau +  $\geq 97.65$  pg/mL, aHPV +  $\leq 6386.85$  mm<sup>3</sup>, and FDG-PET +  $\leq 1.1495$ . Secondly, a biomarker classification was done via the receiver operating characteristics (ROC) analyses (see “Statistical analyses” section), which produced the new cutoff values: CSF t-tau +  $\geq 68.65$  pg/mL, aHPV +  $\leq 6586.14$  mm<sup>3</sup>, and FDG-PET +  $\leq 1.1776$ .

The subjects were then categorized into three groups depending on the status of neurodegenerative biomarkers: CSF/PET group (CSF-/PET-, CSF-/PET+, CSF+/PET-, and CSF+/PET+), CSF/MRI group (CSF-/MRI-, CSF-/MRI+, CSF+/MRI-, and CSF+/MRI+), and PET/MRI group (PET-/MRI-, PET-/MRI+, PET+/MRI-, and PET+/MRI+). Besides, according to the discordance and concordance of CSF and imaging biomarkers, we further categorized the participants into concordant-negative, discordant, and concordant-positive groups.

## Statistical analyses

We tested group differences using the Kruskal–Wallis analyses for continuous variables and chi-square tests for categorical data. Continuous variables were presented as means (standard deviations (SDs)) and categorical variables as numbers (percents). Cognitive scores and brain volumes were  $z$  log-transformed to normalize the distributions, and their longitudinal changes were performed in linear mixed-effects models. The models had random intercepts, slopes for time, and an unstructured covariance matrix for the random effects, and included the interaction between time and cognitive score or brain volume as the predictor. In the analyses for cognitive scores, we adjusted for baseline age, gender, *APOE*  $\epsilon 4$ , and years of education. In the analyses for brain volumes, baseline

age, gender, *APOE*  $\epsilon 4$ , and TIV were included as covariates. To access the risk of clinical disease progression (cognitive decline), we constructed unadjusted Kaplan–Meier plots. Progressive cognitive deterioration was defined as: (1) CN subjects converted to MCI or AD; (2) MCI subjects developed to AD at follow-up. Then, we ran multivariate Cox proportional hazard models adjusted for baseline age, gender, educational years, and *APOE*  $\epsilon 4$  status. Besides, we conducted subgroup analyses by clinical diagnosis (CN/MCI). To explore the influence of pathologic changes in AD, we constricted the population to A+T+ and replicated the above longitudinal analyses. In ROC analyses, the maximum value of the Youden’s index (sensitivity + specificity – 1) was defined as the new cutoff point, which could best distinguish CN from AD individuals (Data used in ROC analyses included AD and CN individuals. The cases were AD population, and the controls were CN subjects). Statistical significance was defined as  $P < 0.05$  (two-sided). Statistical analyses were completed using R software (version 3.5.1) and IBM SPSS Statistics 25.

## Results

### Baseline characteristics

This study included 721 subjects (CN = 279, MCI = 442) without removing borderline cases (cutoffs: CSF t-tau +  $\geq 93$  pg/mL; aHPV +  $\leq 6723$  mm<sup>3</sup>; and FDG-PET +  $\leq 1.21$ ) (Table 1). The mean (SD) age of the participants was 72.5 (6.8) years, 46.5% were women, and 98.1% had more than 12 years of education. The follow-up time ranged from 3 months to 14 years. By applying the previously proposed cutoffs, the classification of subjects resulted in three groups (Fig. 1): CSF/PET group (394 CSF-/PET-, 126 CSF-/PET+, 112 CSF+/PET-, 89

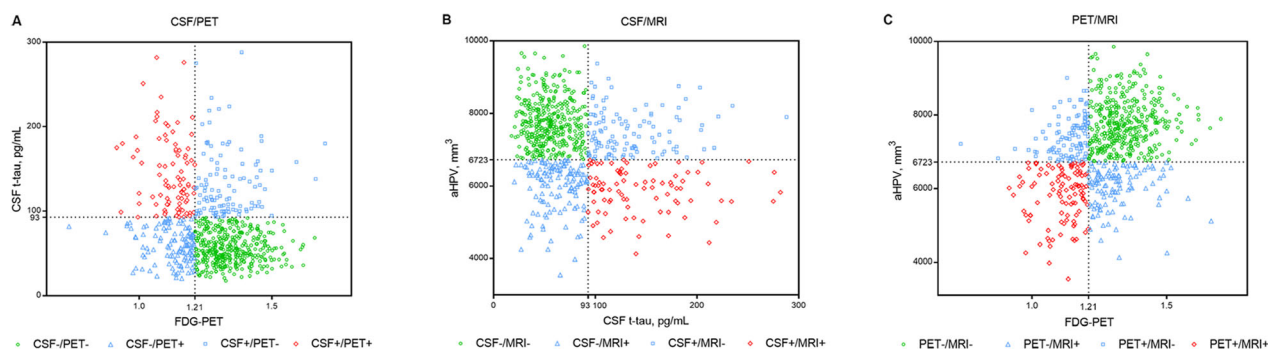


**Figure 1.** Distribution plots of neurodegenerative biomarkers. (A) CSF/PET group: CSF t-tau versus FDG-PET; (B) CSF/MRI group: CSF t-tau versus aHPV; (C) PET/MRI group: FDG-PET versus aHPV. Dashed lines represent the cutoff values for CSF t-tau, FDG-PET, and aHPV. Abbreviations: aHPV, adjusted hippocampal volume; CSF, cerebrospinal fluid; FDG, <sup>18</sup>F-fluorodeoxyglucose; MRI, Magnetic Resonance Imaging; PET, positron emission tomography; t-tau, total tau.

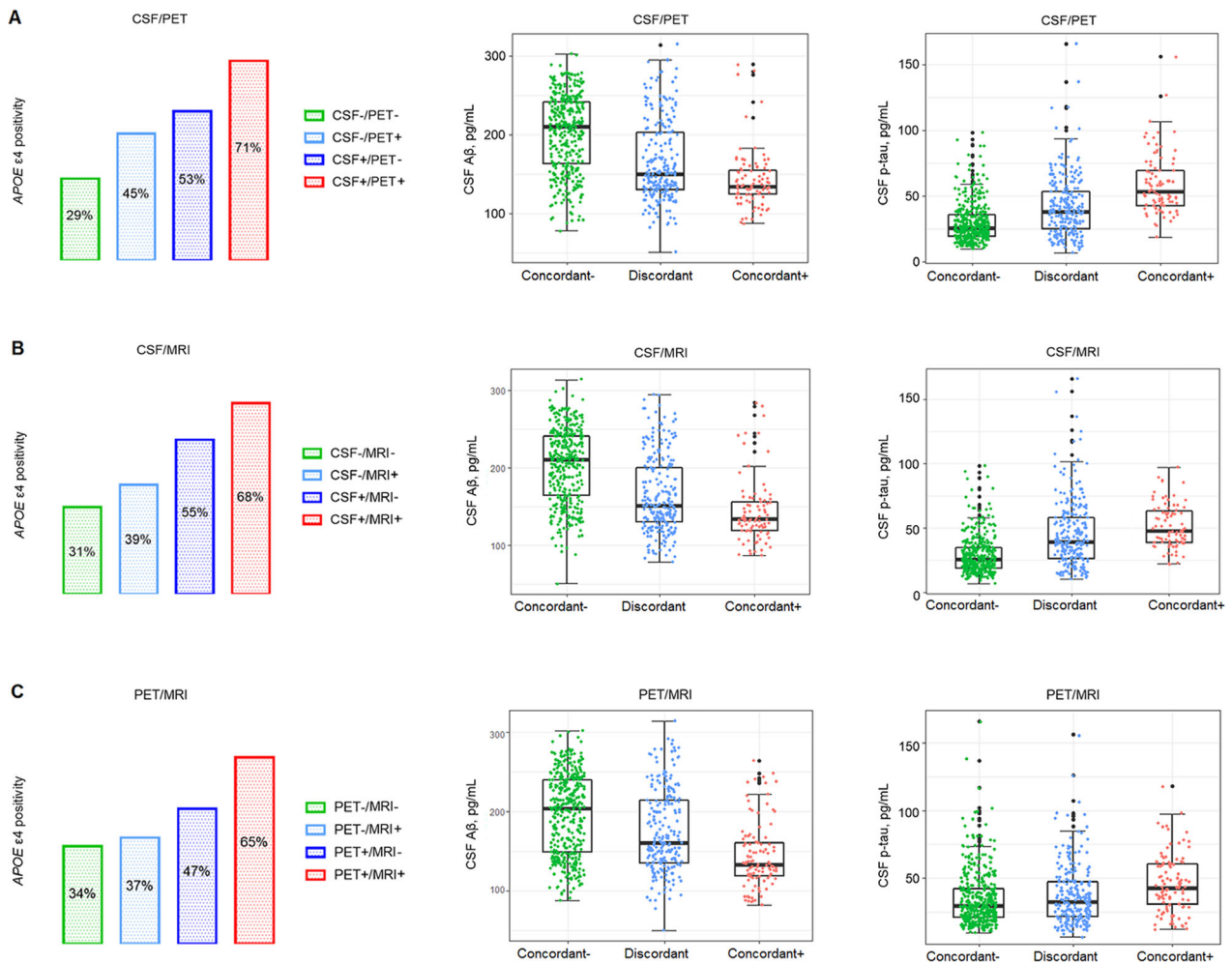


**Figure 2.** Differences in *APOE*  $\epsilon 4$  positivity, CSF  $A\beta 42$ , and p-tau levels. (A) CSF/PET group; (B) CSF/MRI group; (C) PET/MRI group. Abbreviations:  $A\beta$ , amyloid beta; CSF, cerebrospinal fluid; MRI, Magnetic Resonance Imaging; PET, positron emission tomography; p-tau, phosphorylated tau.

CSF+/PET+), CSF/MRI group (387 CSF-/MRI-, 133 CSF-/MRI+, 114 CSF+/MRI-, 87 CSF+/MRI+), and PET/MRI group (392 PET-/MRI-, 114 PET-/MRI+, 109 PET+/MRI-, 106 PET+/MRI+). Distribution of clinical diagnosis (CN/MCI), age, *APOE*  $\epsilon 4$  positivity, MMSE, CDRSB, FAQ, aHPV, entorhinal volume, whole brain volume, FDG-PET, CSF  $A\beta 42$ , p-tau, and t-tau were significantly different among concordant and discordant individuals in the three groups (Appendix S2). Demographic information of A+T+ patients was summarized in Appendix S3. Distribution plots of neurodegenerative biomarkers in A+T+, CN, and MCI individuals were shown in Appendix S4.

The distribution plots of *APOE*  $\epsilon 4$ , CSF  $A\beta 42$ , and p-tau were shown in Figure 2. There was an increase in the proportion of *APOE*  $\epsilon 4$  positivity from concordant-negative to discordant to concordant-positive in the three

groups. The *APOE*  $\epsilon 4$  allele frequency differed between CSF-/MRI+ and CSF+/MRI- groups (39% vs. 55%,  $P = 0.011$ ), whereas no significant differences were detected between PET-/MRI+ and PET+/MRI- groups. The trend was similar in CSF p-tau in the three groups, as discordant patients had more CSF p-tau accumulations than concordant-negative individuals and concordant-positive subjects had more CSF p-tau deposits than discordant patients. There were significant differences in CSF p-tau burden between CSF+/PET- and CSF-/PET+ groups as well as between CSF+/MRI- and CSF-/MRI+ groups (both  $P < 0.001$ ). Additionally, the concentration of CSF  $A\beta 42$  reduced from concordant-negative to discordant to concordant-positive in the three groups. CSF+/PET- and CSF+/MRI- patients showed lower CSF  $A\beta 42$  levels than CSF-/PET+ and CSF-/MRI+ patients, respectively (both  $P = 0.006$ ).

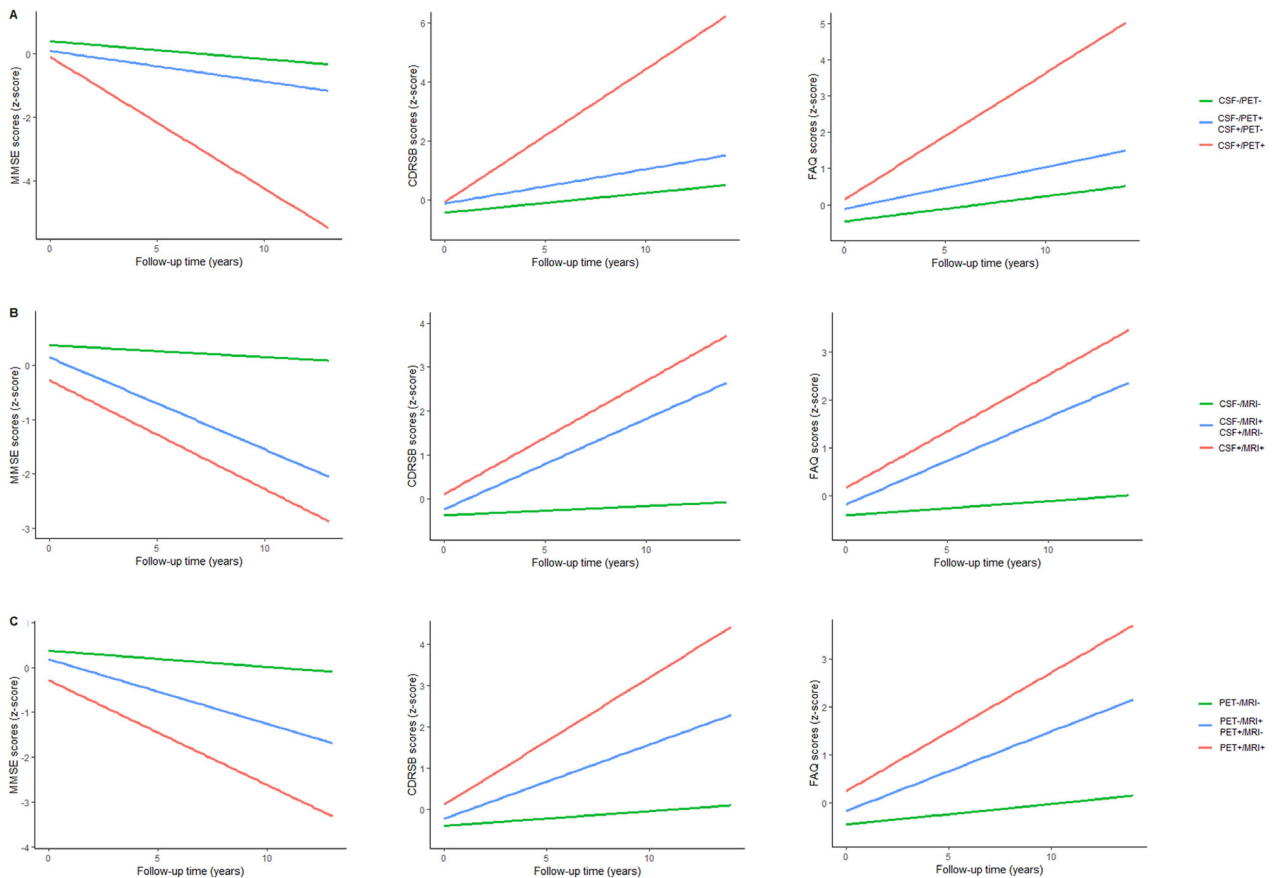


**Figure 3.** Longitudinal changes of cognitive scores in different groups. (A) CSF/PET group; (B) CSF/MRI group; (C) PET/MRI group. In the three groups, we found that the declining rates of MMSE scores showed a downward trend, while the rising rates of CDRSB and FAQ scores showed an upward trend, from concordant-negative to discordant to concordant-positive. Abbreviations: CDRSB, Clinical Dementia Rating Scale-Sum of Boxes; CSF, cerebrospinal fluid; FAQ, Functional Activities Questionnaire; MMSE, Mini-Mental State Examination; MRI, Magnetic Resonance Imaging; PET, positron emission tomography.

### Longitudinal Changes in cognitive scores and brain structures

In the longitudinal analyses of cognitive scores (Fig. 3), we adjusted for age, gender, *APOE*  $\epsilon 4$ , and years of education at baseline. In terms of MMSE score over time, discordant group performed better than concordant-positive group ( $P < 0.0001$ ), and demonstrated an accelerated decline than concordant-negative group ( $P < 0.0001$ ). MMSE scores declined faster in CSF-/PET+ patients than CSF+/PET- patients ( $P = 0.0406$ ), and there were no differences in MMSE scores between CSF-/MRI+ and CSF+/MRI- patients, as well as between PET-/MRI+ and PET+/MRI- patients. There was an upward trend in the rising rates of CDRSB and FAQ scores from concordant-negative to discordant to concordant-positive in CSF/PET, CSF/MRI, and PET/MRI groups. CSF+/PET-

patients had a faster accrual of FAQ scores than CSF-/PET+ patients ( $P = 0.0020$ ) (Appendices S5 and S6). In subgroup analyses, MCI patients who had more abnormal “N” biomarkers performed worse over time on various cognitive assessments (MMSE, CDRSB, and FAQ) in CSF/PET, CSF/MRI, and PET/MRI groups. Concerning CN subjects, this tendency was only significant in CDRSB scores (Appendix S7).

In the longitudinal analyses of brain structures (Fig. 4), we adjusted for age, gender, *APOE*  $\epsilon 4$ , and TIV at baseline. There was an elevated tendency for the rates of deterioration of hippocampal, entorhinal, and whole brain structures from concordant-negative to discordant to concordant-positive in CSF/PET, CSF/MRI, and PET/MRI groups. CSF+/PET- patients had faster rates of hippocampal atrophy than CSF-/PET+ patients ( $P = 0.0474$ ). However, no group differences were detected in entorhinal or

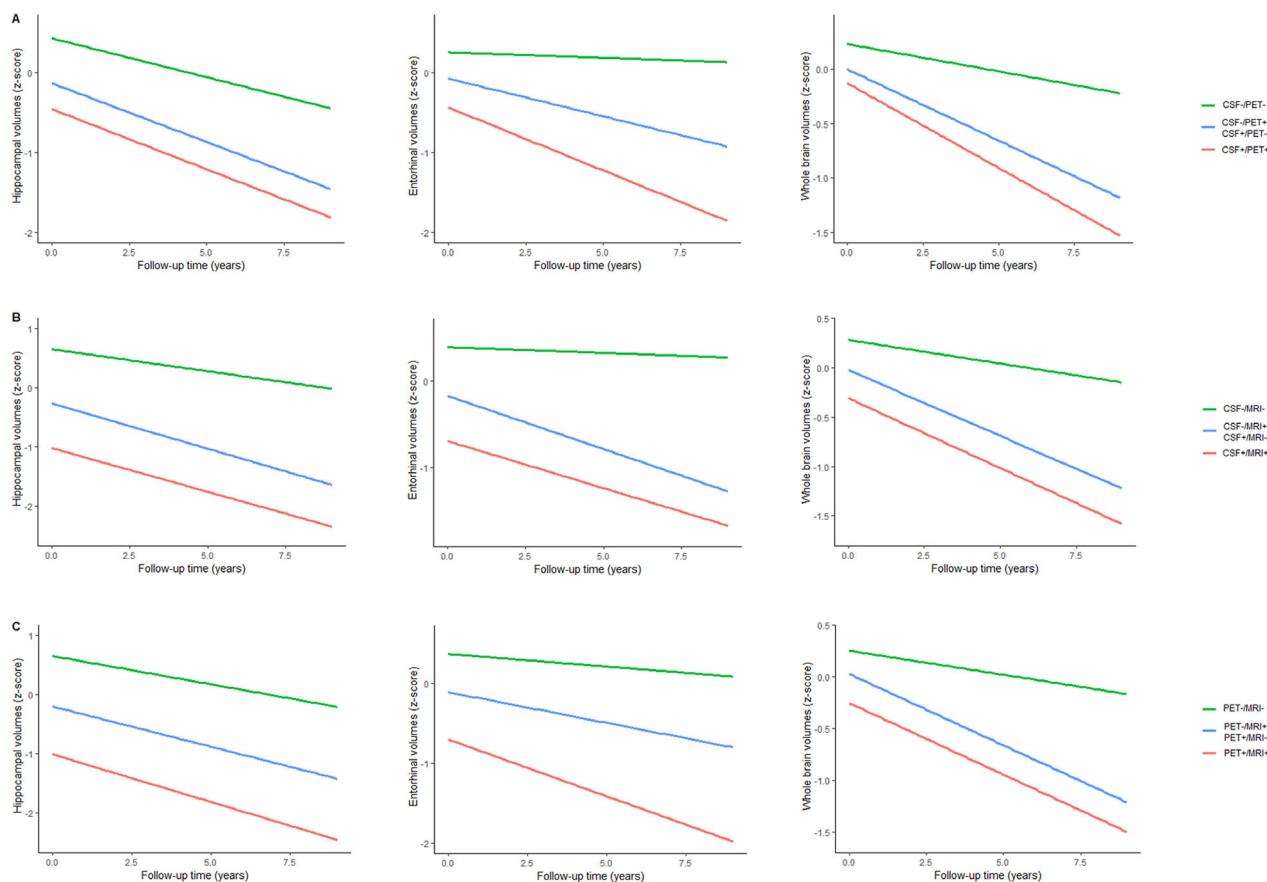


**Figure 4.** Longitudinal changes of brain volumes in different groups. (A) CSF/PET group; (B) CSF/MRI group; (C) PET/MRI group. There was an upward tendency for the rates of deterioration of hippocampal, entorhinal, and whole brain structures from concordant-negative to discordant to concordant-positive in the three groups. Abbreviations: CSF, cerebrospinal fluid; MRI, Magnetic Resonance Imaging; PET, positron emission tomography.

whole brain atrophy rates among discordant subjects (Appendices S5 and S6). In subgroup analyses, MCI patients who had more abnormal “N” biomarkers displayed accelerated reductions in brain volumes in CSF/PET, CSF/MRI, and PET/MRI groups. As for CN subjects, hippocampal atrophy rates were greater in the CSF+/PET+ group than the discordant group (CSF-/PET+ or CSF+/PET-), and entorhinal atrophy rates were greater in the discordant group (CSF-/MRI+ or CSF+/MRI-) than the CSF-/MRI- group (Appendix S7).

In A+T+ patients, cognitive performance in cognitive scores (MMSE, CDRSB, and FAQ) worsened from concordant-negative to discordant to concordant-negative. In terms of brain structures (hippocampus, entorhinal cortex, and whole brain), the discordant group (CSF-/MRI+ or CSF+/MRI-) displayed higher atrophy rates than the CSF-/MRI- group, and the PET+/MRI+ group showed elevated atrophy rates than the discordant group (PET-/MRI+ or PET+/MRI-). Moreover, hippocampus and whole brain atrophied faster in the discordant group

(CSF-/PET+ or CSF+/PET-), compared with the CSF-/PET- group (Appendices S8 and S9).

### Analyses of clinical progression

In Cox regression models, we adjusted for age, gender, educational level, and *APOE*  $\epsilon 4$  status. The conversion risk in the CSF+/PET+ group was 2.6147 times higher than that of the discordant group (CSF-/PET+ or CSF+/PET-), and the risk within the discordant group was 3.3275 times higher than that in the CSF-/PET- group. Discordant patients within CSF/MRI group had a greater conversion rate than CSF-/MRI- individuals (HR = 4.0255, 95% CI = 2.8093–5.7680), and CSF+/MRI+ patients progressed faster compared with discordant individuals (HR = 2.0081, 95% CI = 1.4338–2.8130). Similarly, discordant patients in PET/MRI group were more likely to progress than those in the PET-/MRI- group with the HR of 3.9705 (95% CI = 2.7735–5.6840), and PET+/MRI+ participants displayed an increased risk of conversion than

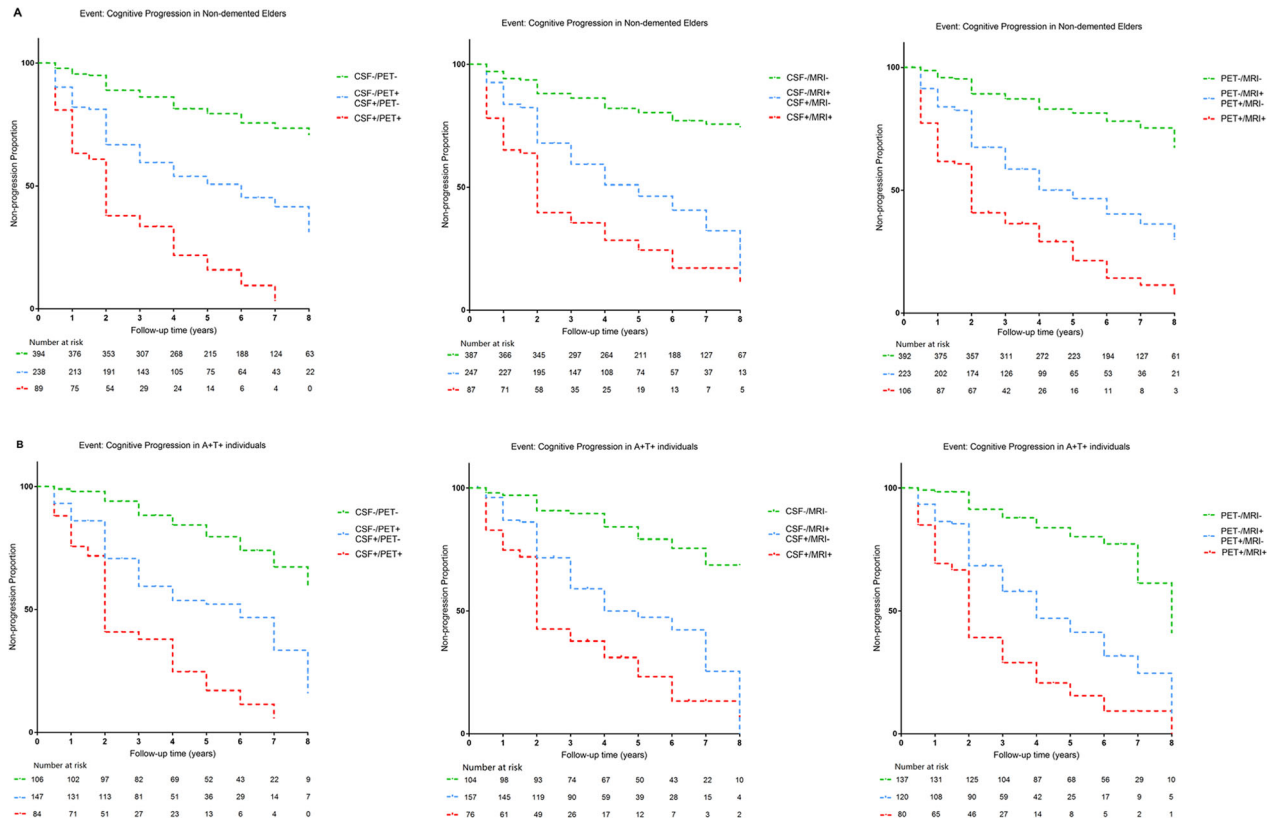


**Figure 5.** Survival analyses for probability of cognitive decline in (A) non-demented elders, and (B) A+T+ individuals. Comparisons of clinical progression (cognitive decline) between concordant and discordant individuals were shown in CSF/PET, CSF/MRI, and PET/MRI groups. Numbers of individuals at risk at different follow-up time points were presented. Survival time was calculated according to the intervals from the baseline evaluation to the time points of clinical progression. Abbreviations: CSF, cerebrospinal fluid; MRI, Magnetic Resonance Imaging; PET, positron emission tomography.

discordant participants with the HR of 1.9915 (95% CI = 1.4366–2.7607) (Fig. 5A, Appendix S10). Besides, we did not detect any intergroup differences in the risk of conversion among discordant patients in CSF/PET, CSF/MRI, and PET/MRI groups (Appendices S11 and S12). Then, we performed subgroup analyses stratified by clinical diagnosis. In MCI patients, the risk of conversion increased from concordant-negative to discordant to concordant-positive in CSF/PET, CSF/MRI, and PET/MRI groups. Nonetheless, among CN subjects, no significant difference was observed in the risk of conversion between discordant and concordant-positive individuals in both CSF/PET and PET/MRI groups. And no significant intergroup differences were detected among discordant subjects in both CN and MCI individuals (Appendices S13 and S14).

In A+T+ patients, the CSF+/PET+ group had a greater risk of progression than the discordant group (CSF-/PET+ or CSF+/PET-) with the HR of 2.3200 (95% CI = 1.6382–3.2856), and the risk of the discordant group

was 3.1766 times that of the CSF-/PET- group. Similarly, in CSF/MRI and PET/MRI groups, discordant subjects progressed faster than concordant-negative subjects, and concordant-positive subjects progressed faster than discordant patients. CSF-/PET+ subjects showed a 2.1276-fold risk of cognitive decline compared with CSF+/PET- participants, and CSF-/MRI+ individuals displayed a 1.6591-fold risk than that of CSF+/MRI- participants (Fig. 5B, Appendices S15 and S16).

### Sensitivity analyses

Sensitivity analyses using other cutoffs and neurodegenerative biomarkers were performed:

1 When applying previously proposed cutoffs by excluding borderline cases (CSF t-tau + ≥97.65 pg/mL, aHPV + ≤6386.85 mm<sup>3</sup>, and FDG-PET + ≤1.1495), 380 individuals were included (Appendices S17 and S18). Patients with more abnormal neurodegenerative biomarkers had a greater risk of cognitive deterioration

in CSF/PET, CSF/MRI, and PET/MRI groups (Appendices S19 and S20). Besides, CSF−/PET+ subjects were more likely to progress than CSF+/PET− individuals.

2 We also used new cutoffs derived from the ROC analyses (CSF t-tau +  $\geq 68.65$  pg/mL, aHPV +  $\leq 6586.14$  mm<sup>3</sup>, and FDG-PET +  $\leq 1.1776$ ) (Appendices S21 and S22). The more abnormal neurodegenerative biomarkers the patients had, the higher progression risk they displayed (Appendices S23 and S24). Besides, CSF−/PET+ and PET+/MRI− participants showed higher progression rates in comparison with CSF+/PET− and PET−/MRI+ individuals, respectively.

3 As an established biomarker of neurodegeneration,<sup>28</sup> plasma neurofilament light was also included (Appendix S25). We found that discordant group was intermediate to concordant-negative and concordant-positive groups in terms of baseline CSF A $\beta$ 42 and p-tau levels, as well as longitudinal rates of cognitive decline and conversion risk. These results did not change our conclusions.

## Discussion

In the present study, we found that the discordant group was intermediate to concordant-negative and concordant-positive groups in terms of APOE  $\epsilon$ 4 positivity, CSF A $\beta$ 42 and p-tau levels at baseline, as well as the rates of cognitive decline reflected by cognitive scores and brain structures. Besides, the risk of cognitive decline increased from concordant-negative to discordant to concordant-positive. These longitudinal results were validated in A+T+, CN, and MCI individuals, and were also validated by applying different cutoffs and neurodegenerative biomarkers. Altogether, our findings suggest that discordant neurodegenerative status points to a stage of cognitive function which is intermediate between concordant-negative and concordant-positive.

Neurodegenerative pathology can be reliably measured in vivo with neuroimaging technology, CSF assessments, or blood tests,<sup>28</sup> but substantial discordance exists when utilizing different methods to evaluate the “N” biomarkers in the same person.<sup>5,12–15</sup> Researchers have compared the prevalence of biologically defined AD with clinically defined probable AD,<sup>29</sup> and evaluated the correspondence between clinical syndromes and biological biomarkers as well as between CSF tau and tau-PET.<sup>30,31</sup> Likewise, they obtained similar but not equivalent results, revealing the importance of recognizing the discordant status. Some mechanisms were possibly helpful in explaining the discordant states. First, discordant cases accounted for a large proportion (> 30%) in the whole study sample, and consequently, differences might exist in the time point at which neurodegenerative changes were detected by

distinct measures. Vemuri et al. reported that MRI could be closer correlated with cognitive development than CSF t-tau, since the latter might be more prone to diurnal physiologic variations, thus revealing transient rather than cumulative damage.<sup>21</sup> Toledo et al. suggested that structural MRI and CSF t-tau measures rather than FDG-PET showed strong predictive value for progression from CN to MCI or AD.<sup>14</sup> However, our results from discordant subjects were inconsistent. Thus, it is difficult to determine the sequence of “N” biomarker abnormality and find which specific “N” biomarker might reflect an earlier pathological stage, which is in line with the recently proposed temporal pattern of AD biomarkers.<sup>28</sup> Further research on this topic is needed. Second, “N” biomarker abnormalities can be caused by neuronal injury in several diseases, and thus, these biomarkers are not specific for neurodegenerative changes in AD. For example, the increased plasma neurofilament light levels are seen not only in AD dementia<sup>32–34</sup> but also in frontotemporal dementia, vascular dementia, and human immunodeficiency virus-associated dementia.<sup>35</sup> Also, in any individual, the proportion of neurodegenerative damage due to AD versus other probable comorbidities (most of which have no extant biomarker) remains unclear.<sup>1</sup> Therefore, the “N” biomarker positivity could be caused by other diseases rather than AD, such as cerebrovascular disease (white matter hyperintensity) and neuroinflammation.<sup>36–38</sup>

Since AD pathology has accumulated for many years before apparent clinical symptoms occur,<sup>39,40</sup> the early identification of non-demented individuals at imminent risk of cognitive impairment would provide insights into intervention as well as new therapy approaches.<sup>41</sup> And the heterogeneity in the definition of neuronal injury is vital to clinical trials using biomarkers for enrollment or as alternative endpoint measures. In all groups, discordant individuals were intermediate to concordant-negative and concordant-positive persons in terms of cognitive performance, no matter in a non-demented (CN and MCI) population, or a separate CN or MCI population. Accordingly, concordant-negative, discordant, and concordant-positive groups were likely to denote meaningfully different stages of cognitive function. Regardless of any abnormality in neuroimaging signatures (patterns of gray matter atrophy on structural MRI or FDG-PET), CSF t-tau measurements, or plasma tests, the isolated “N” positivity reflected a relatively early stage that needed to implement interventions before any two biomarkers became abnormal. Previous studies have reported the correlations between neuronal injury factors, and it has been noted that the combination of these biomarkers might provide better prediction than either source of data alone.<sup>14,19,21,22</sup> Vos et al. also suggested that individuals

with both CSF A $\beta$  deposition and neuronal injury showed an increased risk of disease progression.<sup>15</sup> These findings emphasize the vital role of discordant biomarkers and the potential utility of integrating multiple modalities in disease.

Our findings may have important implications for the diagnosis and treatment of AD, since they highlight the role of a discordant status in determining the therapeutic window before irreversible neurodegenerative changes occur in AD. In the ATN system, “A” and “T” biomarkers reveal characteristic pathological changes that define AD, whereas neurodegenerative/neuronal injury biomarkers are nonspecific, which are applied only for the staging of disease severity.<sup>1</sup> Targeting A+T+ patients, a recent study has compared the clinical outcomes of individuals having normal or abnormal single “N” biomarker and has found that all of the three “N” biomarkers were highly related to an increased risk of conversion to AD dementia.<sup>42</sup> By combining these “N” biomarkers, our study revealed that the conversion risk in discordant group was intermediate between those of concordant-negative and concordant-positive groups. In another word, even among the patients who have developed into a stage which could be biologically defined as AD (A+T+),<sup>1</sup> dividing patients into N0/N1/N2 subgroups may provide vital prognostic insights on a single-patient scale. As a complement to the original ATN framework, N+ subgrouping could help identify early cognitive deficits and promote disease-modifying therapeutics or interventions of modifiable risk factors, which thus might delay the occurrence of cognitive decline or disease progression. Our work could provide support for the refinement of ATN classification.

This is a large prospective study with a relatively long follow-up duration, which well characterized the cognitive trajectories of discordant and concordant individuals. An additional strength was that results were robust even after threshold modification, or in different populations. Nonetheless, some caveats should be emphasized. First, as the Alzheimer’s continuum exists, dichotomizing each biomarker may mask the continuum. Besides, dichotomizing biomarkers may lead to loss of important prognostic information.<sup>43</sup> Second, although the total sample size was large, the numbers of individuals in various subgroups were insufficient, especially when the discordant population was further categorized into different groups or when groups were stratified by clinical diagnosis, which may reduce the statistical power to detect longitudinal changes. Third, the sample size restricted us to divide the A+T+ group into CN A+T+ and MCI A+T+ groups. For example, among CN A+T+ individuals, the PET+/MRI+ group included only five subjects. Likewise, we did not explore the potential role of white matter lesions on cognitive function due to the small number of people having relevant data.

Fourth, our results targeting discordant subjects were inconsistent and it is difficult to conclude which “N” biomarker became abnormal first. Thus, further investigations targeting this topic were necessary.

In conclusion, this study supported that discordant neurodegenerative status denoted a stage of cognitive function intermediate between concordant-negative and concordant-positive. Identification of discordant cases would provide insights into intervention and disease-modifying therapeutics, particularly in A+T+ individuals. And this work could be a complement to the ATN framework. Moreover, further well-designed studies with sample enrichment are warranted.

## Acknowledgment

This study was supported by grants from the National Key R&D Program of China (2018YFC1314700), the National Natural Science Foundation of China (91849126), Shanghai Municipal Science and Technology Major Project (No.2018SHZDZX03) and ZJlab, Tianqiao and Chrissy Chen Institute, and the State Key Laboratory of Neurobiology and Frontiers Center for Brain Science of Ministry of Education, Fudan University. Data collection and sharing for this project were funded by the Alzheimer’s Disease Neuroimaging Initiative (ADNI) (National Institutes of Health Grant U01 AG024904) and DOD ADNI (Department of Defense award number W81XWH-12-2-0012). ADNI is funded by the National Institute on Aging, the National Institute of Biomedical Imaging and Bioengineering, and through generous contributions from the following: AbbVie, Alzheimer’s Association; Alzheimer’s Drug Discovery Foundation; Araclon Biotech; BioClinica, Inc.; Biogen; Bristol-Myers Squibb Company; CereSpir, Inc.; Cogstate; Eisai Inc.; Elan Pharmaceuticals, Inc.; Eli Lilly and Company; EuroImmun; F. Hoffmann-La Roche Ltd and its affiliated company Genentech, Inc.; Fujirebio; GE Healthcare; IXICO Ltd.; Janssen Alzheimer Immunotherapy Research & Development, LLC.; Johnson & Johnson Pharmaceutical Research & Development LLC.; Lumosity; Lundbeck; Merck & Co., Inc.; Meso Scale Diagnostics, LLC.; NeuroRx Research; Neurotrack Technologies; Novartis Pharmaceuticals Corporation; Pfizer Inc.; Piramal Imaging; Servier; Takeda Pharmaceutical Company; and Transition Therapeutics. The Canadian Institutes of Health Research is providing funds to support ADNI clinical sites in Canada. Private sector contributions are facilitated by the Foundation for the National Institutes of Health ([www.fnih.org](http://www.fnih.org)). The grantee organization is the Northern California Institute for Research and Education, and the study is coordinated by the Alzheimer’s Therapeutic Research Institute at the University of Southern California. ADNI data are

disseminated by the Laboratory for Neuro Imaging at the University of Southern California.

## Authors' Contributions

JTY conceptualized and designed the study. YG, HQL, and LT did the manuscript preparation and data acquisition. YG, HQL, LT, and JTY analyzed the data, performed statistical analysis, and interpreted the data. YG, HQL, LT, SDC, YXY, YHM, and JTY wrote the first draft of the manuscript. All authors reviewed the manuscript. All authors have contributed to the manuscript revising and editing critically for important intellectual content and given final approval of the version and agreed to be accountable for all aspects of the work presented here. All authors read and approved the final manuscript.

## Conflict of Interest

The authors declared no potential conflicts of interest with respect to the research, authorship, and/or publication of this article.

## REFERENCES

- Jack CR Jr, Bennett DA, Blennow K, et al. NIA-AA Research Framework: toward a biological definition of Alzheimer's disease. *Alzheimers Dement* 2018;14:535–562.
- Terry RD, Masliah E, Salmon DP, et al. Physical basis of cognitive alterations in Alzheimer's disease: synapse loss is the major correlate of cognitive impairment. *Ann Neurol* 1991;30:572–580.
- Blennow K, Hampel H. CSF markers for incipient Alzheimer's disease. *Lancet Neurol* 2003;2:605–613.
- Illan-Gala I, Pegueroles J, Montal V, et al. Challenges associated with biomarker-based classification systems for Alzheimer's disease. *Alzheimer's Dement* 2018;10:346–357.
- Alexopoulos P, Kriett L, Haller B, et al. Limited agreement between biomarkers of neuronal injury at different stages of Alzheimer's disease. *Alzheimers Dement* 2014;10:684–689.
- Buchhave P, Minthon L, Zetterberg H, et al. Cerebrospinal fluid levels of beta-amyloid 1–42, but not of tau, are fully changed already 5 to 10 years before the onset of Alzheimer dementia. *Arch Gen Psychiatry* 2012;69:98–106.
- van Rossum IA, Vos SJ, Burns L, et al. Injury markers predict time to dementia in subjects with MCI and amyloid pathology. *Neurology* 2012;79:1809–1816.
- Roe CM, Fagan AM, Grant EA, et al. Amyloid imaging and CSF biomarkers in predicting cognitive impairment up to 7.5 years later. *Neurology* 2013;80:1784–1791.
- Bobinski M, de Leon MJ, Wegiel J, et al. The histological validation of post mortem magnetic resonance imaging-determined hippocampal volume in Alzheimer's disease. *Neuroscience* 2000;95:721–725.
- Zarow C, Vinters HV, Ellis WG, et al. Correlates of hippocampal neuron number in Alzheimer's disease and ischemic vascular dementia. *Ann Neurol* 2005;57:896–903.
- Barkhof F, Polvikoski TM, van Straaten EC, et al. The significance of medial temporal lobe atrophy: a postmortem MRI study in the very old. *Neurology* 2007;69:1521–1527.
- Chetelat G, Ossenkoppele R, Villemagne VL, et al. Atrophy, hypometabolism and clinical trajectories in patients with amyloid-negative Alzheimer's disease. *Brain* 2016;139(Pt 9):2528–2539.
- Gordon BA, Friedrichsen K, Brier M, et al. The relationship between cerebrospinal fluid markers of Alzheimer pathology and positron emission tomography tau imaging. *Brain* 2016;139(Pt 8):2249–2260.
- Toledo JB, Weiner MW, Wolk DA, et al. Neuronal injury biomarkers and prognosis in ADNI subjects with normal cognition. *Acta Neuropathol Commun* 2014;6:26.
- Vos SJB, Gordon BA, Su Y, et al. NIA-AA staging of preclinical Alzheimer disease: discordance and concordance of CSF and imaging biomarkers. *Neurobiol Aging* 2016;44:1–8.
- de Wilde A, Reimand J, Teunissen CE, et al. Discordant amyloid-beta PET and CSF biomarkers and its clinical consequences. *Alzheimers Res Ther* 2019;11:78.
- Palmqvist S, Mattsson N, Hansson O; Alzheimer's Disease Neuroimaging I. Cerebrospinal fluid analysis detects cerebral amyloid-beta accumulation earlier than positron emission tomography. *Brain* 2016;139(Pt 4):1226–1236.
- Rubi S, Noguera A, Tarongi S, et al. Concordance between brain (18)F-FDG PET and cerebrospinal fluid biomarkers in diagnosing Alzheimer's disease. *Rev Esp Med Nucl Imagen Mol* 2018;37:3–8.
- Chiaravalloti A, Barbagallo G, Ricci M, et al. Brain metabolic correlates of CSF Tau protein in a large cohort of Alzheimer's disease patients: a CSF and FDG PET study. *Brain Res* 2018;1:116–122.
- Caminiti SP, Ballarini T, Sala A, et al. FDG-PET and CSF biomarker accuracy in prediction of conversion to different dementias in a large multicentre MCI cohort. *Neuroimage Clin* 2018;18:167–177.
- Vemuri P, Wiste HJ, Weigand SD, et al. MRI and CSF biomarkers in normal, MCI, and AD subjects: diagnostic discrimination and cognitive correlations. *Neurology* 2009;73:287–293.
- Ottoy J, Niemantsverdriet E, Verhaeghe J, et al. Association of short-term cognitive decline and MCI-to-AD dementia conversion with CSF, MRI, amyloid- and (18)F-FDG-PET imaging. *Neuroimage Clin* 2019;22:101771.
- Petersen RC, Aisen PS, Beckett LA, et al. Alzheimer's Disease Neuroimaging Initiative (ADNI): clinical characterization. *Neurology* 2010;74:201–209.
- Saykin AJ, Shen L, Foroud TM, et al. Alzheimer's Disease Neuroimaging Initiative biomarkers as quantitative

- phenotypes: genetics core aims, progress, and plans. *Alzheimers Dement* 2010;6:265–273.
25. Shaw LM, Vanderstichele H, Knapik-Czajka M, et al. Cerebrospinal fluid biomarker signature in Alzheimer's disease neuroimaging initiative subjects. *Ann Neurol* 2009;65:403–413.
  26. Mormino EC, Betensky RA, Hedden T, et al. Synergistic effect of beta-amyloid and neurodegeneration on cognitive decline in clinically normal individuals. *JAMA Neurol* 2014;71:1379–1385.
  27. Jagust WJ, Landau SM, Shaw LM, et al. Relationships between biomarkers in aging and dementia. *Neurology* 2009;73:1193–1199.
  28. Zetterberg H, Bendlin BB. Biomarkers for Alzheimer's disease—preparing for a new era of disease-modifying therapies. *Mol Psychiatry* 2020.
  29. Jack CR Jr, Therneau TM, Weigand SD, et al. Prevalence of biologically vs clinically defined alzheimer spectrum entities using the National Institute on Aging-Alzheimer's Association research framework. *JAMA Neurol* 2019; 76, 1174–1183.
  30. Carandini T, Arighi A, Sacchi L, et al. Testing the 2018 NIA-AA research framework in a retrospective large cohort of patients with cognitive impairment: from biological biomarkers to clinical syndromes. *Alzheimers Res Ther* 2019;11:84.
  31. Scholl M, Maass A, Mattsson N, et al. Biomarkers for tau pathology. *Mol Cell Neurosci* 2019;97:18–33.
  32. Mattsson N, Cullen NC, Andreasson U, et al. Association between longitudinal plasma neurofilament light and neurodegeneration in patients with Alzheimer disease. *JAMA Neurol* 2019;76:791–799.
  33. Preische O, Schultz SA, Apel A, et al. Serum neurofilament dynamics predicts neurodegeneration and clinical progression in presymptomatic Alzheimer's disease. *Nat Med* 2019;25:277–283.
  34. Weston PSJ, Poole T, O'Connor A, et al. Longitudinal measurement of serum neurofilament light in presymptomatic familial Alzheimer's disease. *Alzheimers Res Ther* 2019;11:19.
  35. Bridel C, van Wieringen WN, Zetterberg H, et al. Diagnostic value of cerebrospinal fluid neurofilament light protein in neurology: a systematic review and meta-analysis. *JAMA Neurol* 2019; 76, 1035–1048.
  36. Bos I, Verhey FR, Ramakers I, et al. Cerebrovascular and amyloid pathology in predementia stages: the relationship with neurodegeneration and cognitive decline. *Alzheimers Res Ther* 2017;9:101.
  37. Soldan A, Pettigrew C, Zhu Y, et al. White matter hyperintensities and CSF Alzheimer disease biomarkers in preclinical Alzheimer disease. *Neurology* 2020; 94, e950–e960.
  38. Niranjana R. Recent advances in the mechanisms of neuroinflammation and their roles in neurodegeneration. *Neurochem Int* 2018;120:13–20.
  39. Price JL, Morris JC. Tangles and plaques in nondemented aging and "preclinical" Alzheimer's disease. *Ann Neurol* 1999;45:358–368.
  40. Sheline YI, Raichle ME. Resting state functional connectivity in preclinical Alzheimer's disease. *Biol Psychiat* 2013;74:340–347.
  41. Meyer PF, Binette AP, Gonneaud J, Breitner JCS, Villeneuve S. Characterization of Alzheimer disease biomarker discrepancies using cerebrospinal fluid phosphorylated tau and AV1451 positron emission tomography. *JAMA Neurol* 2020;77:508.
  42. Ou YN, Xu W, Li JQ, et al. FDG-PET as an independent biomarker for Alzheimer's biological diagnosis: a longitudinal study. *Alzheimers Res Ther* 2019;11:57.
  43. Mattsson-Carlgen N, Leuzy A, Janelidze S, et al. The implications of different approaches to define AT(N) in Alzheimer disease. *Neurology* 2020;94:e2233–e2244.

## Supporting Information

Additional supporting information may be found online in the Supporting Information section at the end of the article.

**Appendix S1.** The excluded borderline values within  $\pm 5\%$  of the original cutoff value.

**Appendix S2.** Results of demographic characteristics among different groups.

**Appendix S3.** Demographic information in A+T+ patients.

**Appendix S4.** Distribution plots of "N" biomarkers in A+T+, CN, and MCI individuals.

**Appendix S5.** Results of longitudinal analyses in brain structures and cognitive scores between discordant and concordant groups.

**Appendix S6.** Results of longitudinal analyses in brain structures and cognitive scores among discordant patients.

**Appendix S7.** Results of longitudinal analyses in brain structures and cognitive scores among CN and MCI individuals.

**Appendix S8.** Longitudinal analyses in brain structures and cognitive scores among A+T+ patients.

**Appendix S9.** Results of longitudinal analyses in brain structures and cognitive scores among A+T+ patients.

**Appendix S10.** Results of survival analyses between discordant and concordant patients.

**Appendix S11.** Kaplan–Meier survival curves for probability of cognitive progression in discordant patients.

**Appendix S12.** Results of survival analyses in discordant patients.

**Appendix S13.** Kaplan–Meier survival curves for probability of cognitive progression in CN or MCI individuals.

**Appendix S14.** Results of survival analyses in CN or MCI individuals.

**Appendix S15.** Kaplan–Meier survival curves for probability of cognitive progression in discordant group among A+T+ patients.

**Appendix S16.** Results of survival analyses in A+T+ patients.

**Appendix S17.** Demographic information with the exclusion of borderline cases.

**Appendix S18.** Distribution plots of “N” biomarkers with the exclusion of borderline cases.

**Appendix S19.** Kaplan–Meier survival curves for probability of cognitive progression when excluding borderline cases.

**Appendix S20.** Results of survival analyses when excluding borderline cases.

**Appendix S21.** Demographic information (cutoffs for neurodegenerative biomarkers were derived from ROC analyses).

**Appendix S22.** Distribution plots (cutoffs for neurodegenerative biomarkers were derived from ROC analyses).

**Appendix S23.** Kaplan–Meier survival curves for probability of cognitive progression (cutoffs for neurodegenerative biomarkers were derived from ROC analyses).

**Appendix S24.** Results of survival analyses (cutoffs for neurodegenerative biomarkers were derived from ROC analyses).

**Appendix S25.** Analyses of plasma neurofilament light.